CHANGES IN DEPTH OF YELLOWFIN TUNA HABITAT IN THE INDIAN OCEAN: AN HISTORICAL PERSPECTIVE 1955-2001

Francis Marsac

IRD, UR 109 'Thetis'

BP 172

97492 Sainte Clotilde

La Réunion

E-mail: marsac@ird.fr

ABSTRACT

This paper is an analysis of the changes affecting the depth of habitat of yellowfin tuna, at interannual time scale, for the period 1955-2001. Two variables are selected to define the habitat: depth of the 20°C isotherm (Z20) that defines the core of the thermocline, and a derived depth of the 2ml/l dissolved oxygen concentration (Zox2) that defines limit conditions to vertical distribution. The Zox2 is deducted from temperature at depth data, using a correlation between temperature and oxygen. Such changes in habitat depth can potentially affect the catchability. There is a clear pattern of variability with out-of-phase fluctuations between East and West of the ocean. During the El Niño warm phase, there is a deepening of the thermocline and Zox2 in the West and a subsequent shoaling in the East. The largest anomalies takes place between 50°E and 70°E (Western Indian Ocean), where major yellowfin fishing grounds for purse seine and longline are located. Two frequency domains are discernable in the time series of both parameters: a quasi-quadriennal oscillation that is likely to be linked to the ENSO dynamics, and a longer cycle around 25 years. No particularly trend is shown on the long-term; however the length of the series is still too short to address interdecadal fluctuations. The year-to-year changes in depth of limit conditions of the yellowfin habitat ranges between 5 and 50 meters.

INTRODUCTION

Yellowfin tuna, at least in its juvenile stage, is mainly distributed within the mixed layer. In the equatorial regions, a well-marked thermocline is found at the bottom of the mixed layer. Sonic tagging has shown that dwelling time of young yellowfin (less than 1 m FL) is distributed about the maximum temperature gradient, within the thermocline (Cayré & Marsac 1993). The oxycline is also limiting the depth distribution (Marsac et al 1996). The limitation in oxygen is critical for high metabolism animals such as tunas, and it is known that the range 2.5-3 ml/l is a threshold for small yellowfin (Sharp & Dizon 1978). The adult fish have a greater tolerance to ambient conditions: they can dive deeper, stay a significant amount of time in cool waters and they can bear lower oxygen concentration than juvenile. However, for young and adult stages, the thermocline remains a layer of high dwelling time. The thermocline often matches with the pycnocline (density barrier) in the equatorial region. It is the place where sedimenting organisms from the surface accumulate, providing food for migrating fauna and surface dwelling predators.

The depth distribution of the fish is also an important parameter that can affect the catchability of tuna to the fishing gears. Studying the variability of the mixed layer and oxygen content at depth can be used to understand changes in depth of the habitat for yellowfin, and the potential vulnerability of the fish to the purse seine gear. In this paper, we focus on the depth of the 20°C (Z20) and the depth at which the 2ml/l oxygen level is found (Zox2). Z20 is often used to define the core of the thermocline, a Zox2 can be considered as a lower boundary limiting depth distribution of yellowfin.

DATA AND METHODS

The analysis is carried out on a temperature-at-depth data set constructed from mechanical (MBTs) and expendable (XBTs) bathythermographs, and from electronic probes (CTDs) collected in the Indian Ocean during the period 1944-2001. The data set was built by the Joint Environmental Data Analysis Center (JEDAC) at Scripps Institution of Oceanography, La Jolla, California (White 2000). Observations matching the quality control tests were pooled by month and 5°longitude-2°latitude. Using an optimal interpolation procedure, temperature at standard levels was calculated from the observed data, in each block and month.

From the temperature-at-depth data, it is possible to obtain Z20 by a simple interpolation in the depth range containing the 20°C isotherm. The Zox2 is derived from the correlation existing between temperature and oxygen in a given depth (and temperature) range. Temperature and oxygen levels vary mostly according to latitude, and then we stratified the Indian Ocean in different latitude belts and computed the correlations within these belts. The results are given in Table 1. The highest correlation is found in the temperature range [18°C-26°C].

In order to describe the pattern of variability of the two variables, empirical orthogonal functions (EOF) are used. The method using EOFs, a technique derived from the principal component analysis has been extensively used in meteorology and oceanography to analyze space and time trends in data sets (Lorenz 1956). The method represents the data as a sum of products of functions: $f(x, y, t) = \sum (F_i(x, y). G_i(x, y)$ where the F_i denote the data distribution in space and the G_i give the contribution of the respective space distribution at any given time. An infinite sum of functions will reproduce the current observations but, practically, the summation is truncated after the first few terms. The contributions of the sum are arranged in such a way that the first term (= first axis) accounts for more of the variance found in the observations than any other term. The second term accounts for most of the remaining variance and so on. The Eigen values that are calculated by this method have no unit and are proportional to deviations about the mean (standardized anomalies). The product of the spatial value (or coefficient) for the grid point (x, y) and the value at time *t* gives the sign of the anomaly for the triplet (x, y, t).

The equatorial region (10°N-10°S) is the core area for yellowfin, as depicted by the distribution of longline and purse seine catches (fig. 1). Higher catches (and catch rates) are obtained in the Western Indian Ocean (west of 70°E) compared to the Eastern IO. The major difference between catch distributions of these fisheries is the existence of significant catches by longline in the North Arabian Sea. However, such levels of catches are not a regular feature as the sole year 1993 represents 42% of the total yellowfin catches made during the period 1986-1998.

For both fisheries, a seasonal pattern is noticeable. In the equatorial region, the yellowfin catches by purse seiners occur mainly from December to March that is during the spawning season. Although juvenile yellowfin can be caught all the year round on FADs, the highest contribution in weight is made during the above mentioned period, when purse seiners exploit free schools of spawners. Longline catches peak from January to May in the equatorial region and in April-May in the Northern Arabian Sea.

RESULTS

Average pattern of the Z20

Mean Z20 for the period 1955-2001 is calculated for January and July (fig. 2). The main features displayed by the figure are:

Shallower Z20 are observed in the Western basin of the ocean compared to the Eastern basin

There is a sharp latitudinal transition between the deep Z20 south of 12°S (> 140 m) and the shallow Z20 (< 100 m) between 0° and 10°S are shallower in the area 0-10°S. The shallower region (< 80 m) corresponds to the divergence between the westward South Equatorial Current and the eastward Equatorial Counter-Current (in January).

The area between 0° and 10°N is clearly distinct from the 0°-10°S.

The Z20 ridge is still observed in the opposite season, but a significant deepening occurs in the Arabian Sea during the Southwest monsoon, in relation with the onset of an anticyclonic gyre.

Average pattern of the derived-Zox2

The derived depth of the 2ml/l dissolved oxygen content is calculated for January only, from 10°S to 24°N (fig. 3). January was selected as it stands within the peak seasons of purse seine and longline catches in the equatorial region. The main features displayed by the figure are:

There is a sharp contrast between the area 0°-5°S with deep Zox2 (> 140 m) and the area 5°S-10°S with shallow Zox2 (< 120 m). The deeper Zox2 correspond to the convergence between the Equatorial Counter Current and the westward North Equatorial current, all across the ocean

The greater constrast is observed in the Western basin

The Northern Indian Ocean, and especially the Arabian Sea and Gulf of Bengal between 5°N and 10°N, have shallower Zox2. This reflects oxygen depleted waters in the subsurface, with sharp oxycline in these regions. Local minimum of Zox2 are observed off Somalia, in the Gulf of Aden and Oman coast.

Patterns of variability

EOF analyses are carried out on Z20 and derived-Zox2 for January. It is designed to depict the interannual variability for this given month. We keep only the first axis of variance. The time component is a series of standard deviation at each time step (here the year). The spatial component displays the field of variability; areas with opposite signs depict out of phase variability. Multiplying the standard deviation (time component) with the spatial loadings gives the absolute standard deviation in the map for this axis of variance.

Z20 (fig. 4)

The first EOF for Z20 explains 26.6 % of the variance of the interannual anomaly field. The time component displays anomalous low values in 1971 and 1999-2001, which could be linked to La-Nina type effects. Anomalous high standard deviation occur in 1964, 1983, 1987 and 1998, and are related to El-Nino warm episodes. On the longer term, the current series suggest a decadal-type cycle, with a period about 25-30 years. The spatial component points out clearly a dipole-like situation north of 10°S. The larger magnitude of the interannual anomalies occurs in the Western basin, along 60°E. During an El Nino warm episode, in January, the present model explains a deepening of the Z20 in the West and a shoaling of Z20 in the East. The standard deviation of the anomaly would be around ±10 meters.

Derived-Zox2 (fig. 5)

The first EOF for derived-Zox2 explains 35.3 % of the variance of the interannual anomaly field. On the overall, the trend of the time component of the Zox2 is similar to that of Z20. However, there are less contrasts in the series, with similar values for negative standard deviation all along the early 70's. The spatial pattern is also very similar to the Z20 component, which is expected as the Zox2 is derived from temperature, and that large-scale vertical oscillation is affecting the first hundred meters of the ocean.

Trends in selected areas

We select 3 areas to analyse the interannual and long term trend of the derived-Zox2: North Arabian Sea (20°N-25°N / 60°E-70°E), North Equator area (0°-5°N / 45°E-70°E) and South Equator area (0°-5°S / 45°E-70°E). Time series are given in Figure 6.

North Arabian Sea

Different cycles seem to occur in this region. From 1958 to 1980, there is a quasi quadriennal oscillation that displays a higher frequency in the period 1980-1990, then again 4-year fluctuations. On the long-term, the smoothed series displays a 25 years period from the 60's to the 80's, then a more continuous decrease since then. However, the current series is not long enough to confirm such decadal oscillation. It is noticeable that the very high 1993 longline catches occurred in a situation where the habitat was becoming deeper, which sounds consistent for operations made by the longline gear.

North and South Equator

A rather regular oscillation about 4-5 years is displayed in these 2 equatorial areas. The long-term oscillation is around 20 years, showing an out-of-phase pattern with that of the North Arabian Sea. The Zox2 is 50 m deeper in the South equator compared to the North Equator.

CONCLUSION

The habitat of the yellowfin deducted from temperature-at-depth data exhibits fluctuations in relation with the El-Nino cycle. If we consider the derived depth of the 2ml/l oxygen content as the floor of the optimal habitat of yellowfin, the magnitude of the changes in depth of the habitat can reach 50 m between an El Nino and a normal year. The largest interannual variability occurs in the western basin, from 15°N to 10°S and 50°E to 70°E. It is noteworthy that this area encompasses the largest catches of yellowfin by longline and purse seine fisheries. The variability pattern analysis points out a dipole-like situation between West and East of the Indian Ocean, with out-of-phase response to interannual anomalies such as that of El Nino.

These results must be kept in mind in analysing the catch-per-unit-effort (CPUE) series. The environmental variability can explain only a part of the variance observed on CPUEs, and might be rather minor compared to the effects of the changes in targeting, selectivity and catchability by the fisheries. However, Z20 and/or derived Zox2 field can be used factors to consider in the CPUE standardisation, and data used in this paper are available for such analysis.

REFERENCES

CAYRÉ, P. & F. MARSAC, 1993: Modelling the yellowfin tuna (*Thunnus albacares*) vertical distribution using sonic tagging results and local environmental parameters. Aquat. Living Resour. 6 : 1-14.

DIZON AND G.G. SHARP, 1978: The Ecophysiology of Tunas.

MARSAC, F., P. CAYRÉ & F. CONAND, 1996: Analysis of small scale movements of yellowfin tuna around fish aggregating devices (FADs) using sonic tagging. In Anganuzzi, A.A, K.A Stobberup & N.J. Webb (eds), Proceedings of the Expert Consultation on Indian Ocean tunas, 6th session, Colombo, Sri Lanka, 25-29 Sept. 1995. Indo-Pacific Tuna Project Collective Volume 9 : 151-159.

WHITE, W.B, 2000: Coupled Rossby waves in the Indian Ocean on interannual timescales. *J. Phys. Oceanogr.*, 30, 2972-2988

Table 1 *– Results of linear correlation between temperature and oxygen (Oxy = b + a.Temp), used to deduct the depth of the 2ml/l oxygen. The temperature range 18°C-26°C contains the most explicit correlation between T and O2.*

The correlation is made from oceanographic stations in the area 30°E-80°E for the period 1906-1994 (GAO database) at given periods: January to March between 10°N and 10°S, March to June north of 10°N

Latitude	a	b	r²	N	Z ox2
20-25 N	0.70599	-13.16	0.871	350	21.47
15-20 N	0.59727	-10.87	0.719	445	21.55
10-15 N	0.63678	-11.35	0.767	697	20.96
5-10 N	0.47883	-7.835	0.71	409	20.54
0-5N	0.31844	-3.879	0.619	555	18.46
0-5S	0.23167	-1.588	0.607	258	15.49
5-10S	0.27701	-2.746	0.695	495	17.13

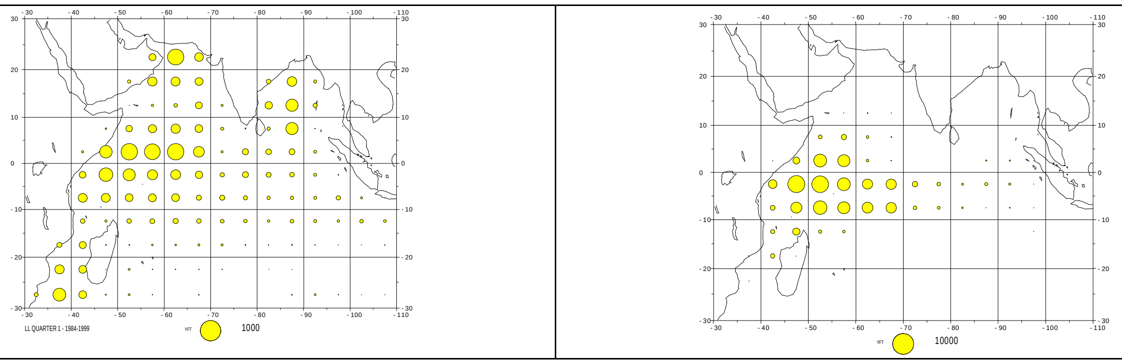

Figure 1 *– Yellowfin catches by 5° square during the first quarter of the year, by the longline (top) and purse seine (bottom) fisheries. Average 1984-1998 for longline (reference circle 1000 t), average 1991-1999 for purse seine (reference circle 10 000 t).*

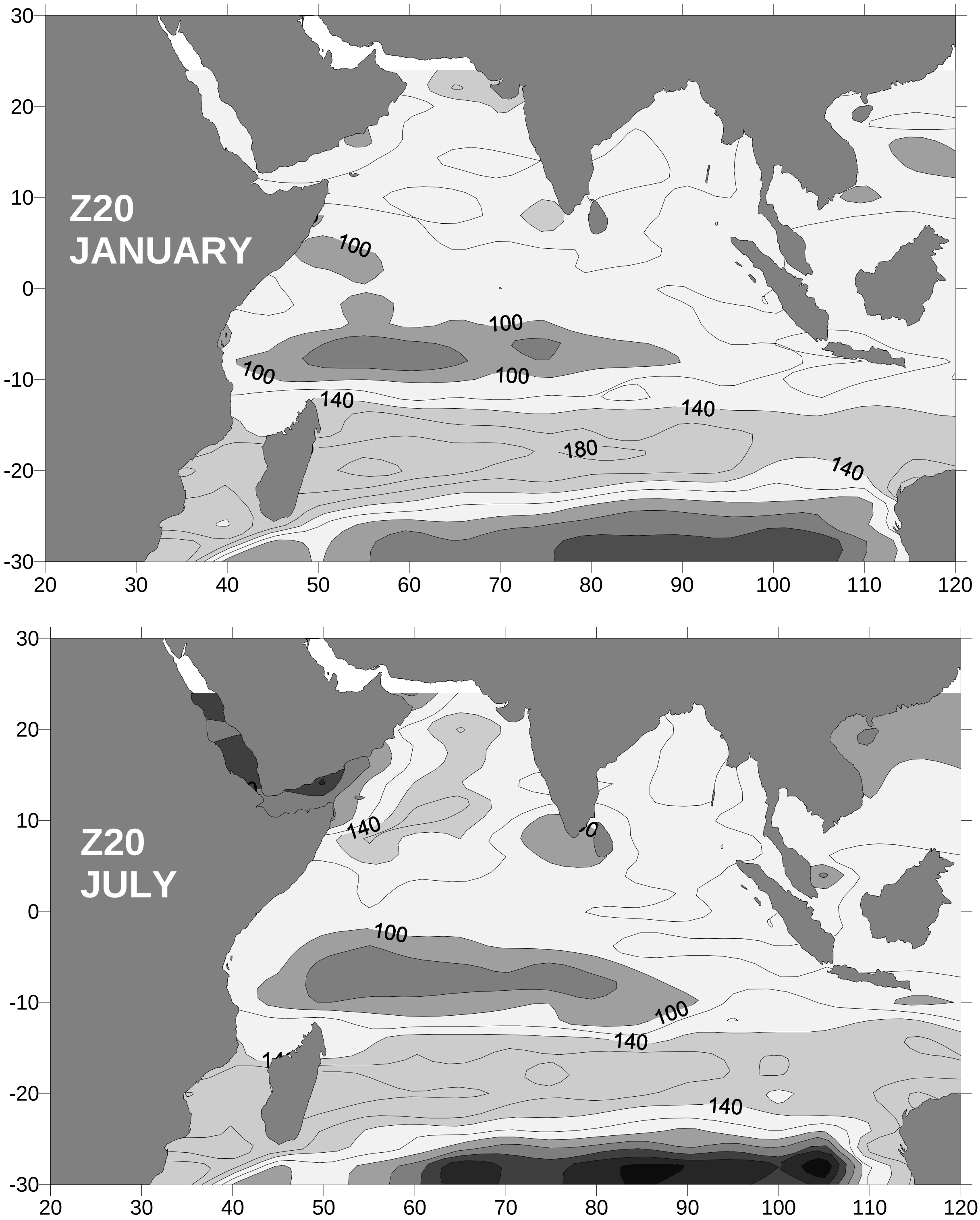

Figure 2 *– Depth of the isotherm 20°C in January and in July. Average 1955-2001. Contour lines every 20 m.*

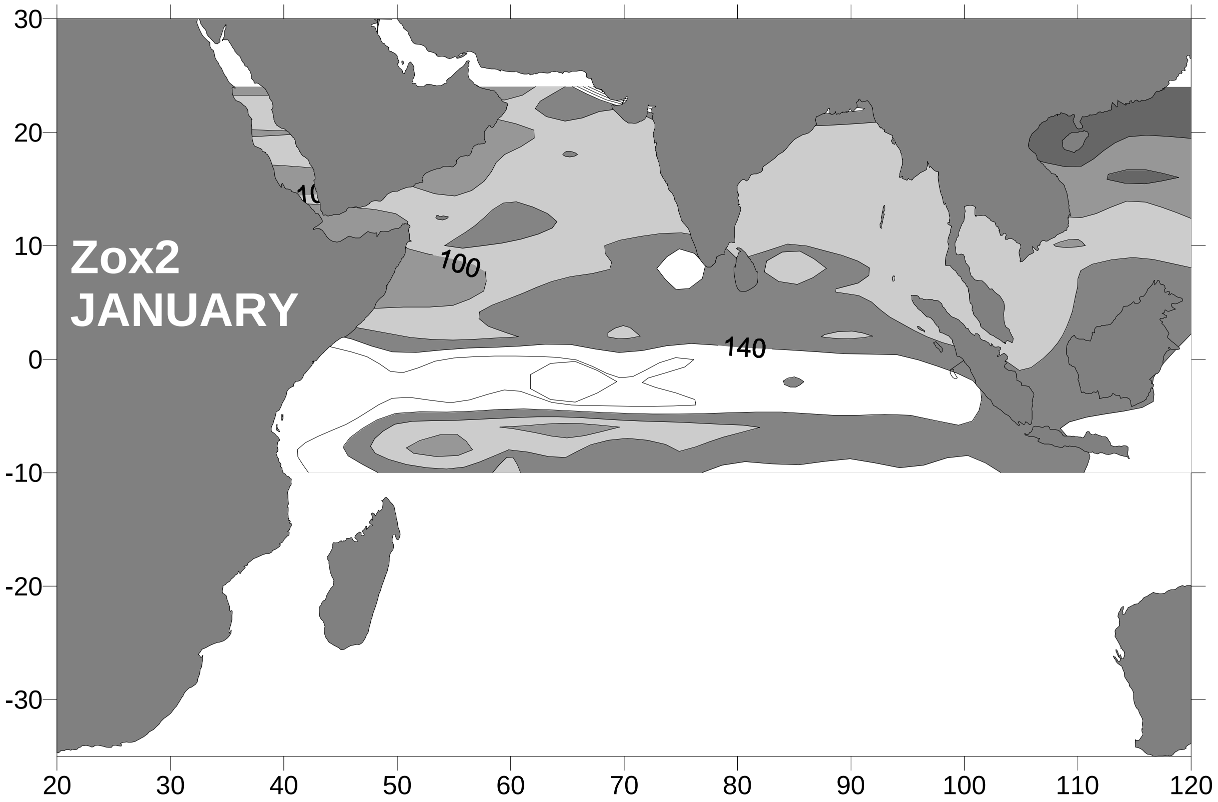

***Figure 3** – Derived depth of the 2ml/l dissolved oxygen content in January. Average 1955-2001. Contour lines every 20 m.*

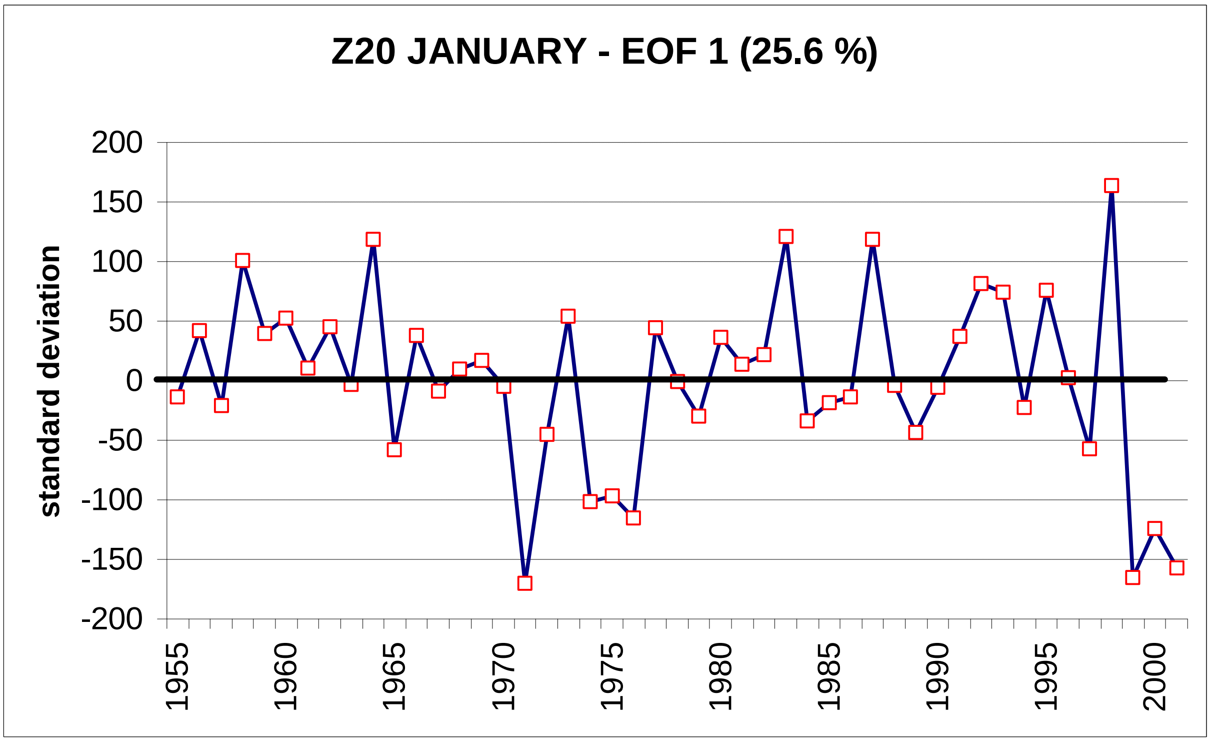

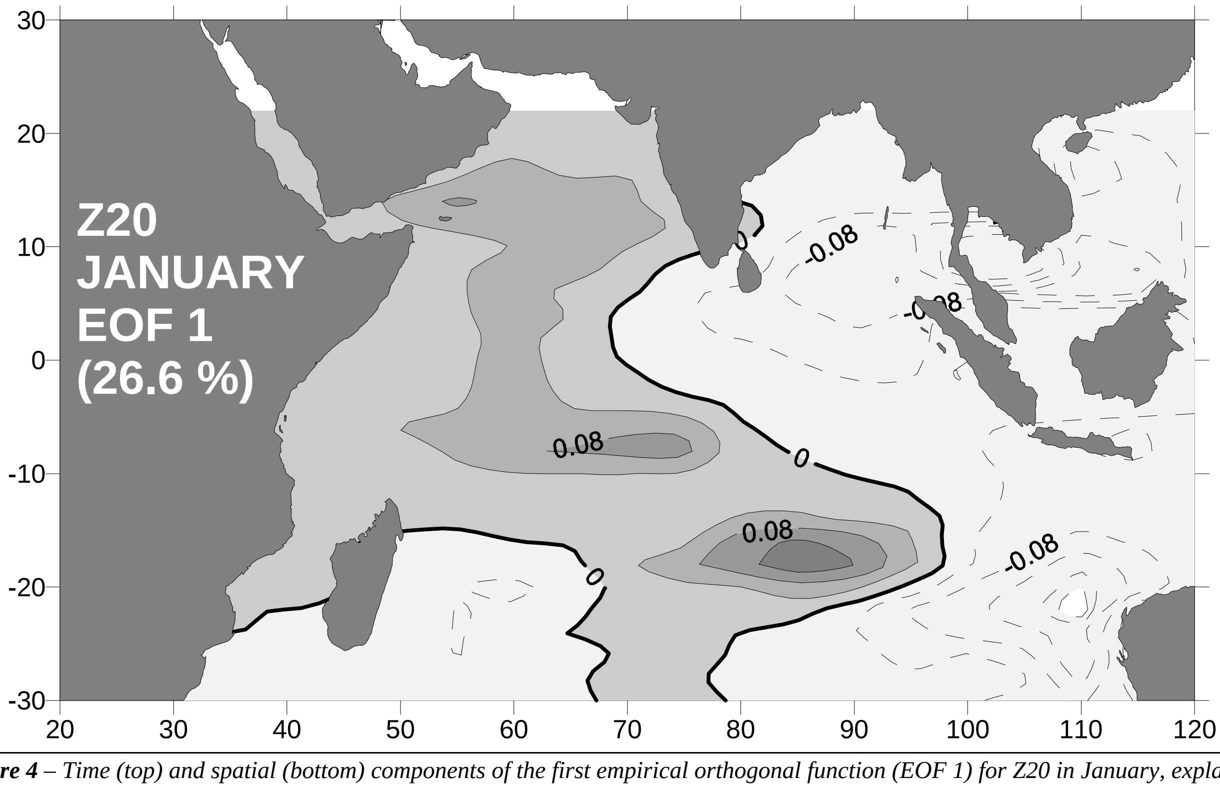

***Figure 4** – Time (top) and spatial (bottom) components of the first empirical orthogonal function (EOF 1) for Z20 in January, explaining 26.6 % of the variance of the anomaly field. This analysis explains the interannual variability for a given month between 1955 and 2001. Note the dipole-like situation north of 10°S, with out of phase (opposite signs) variability between West and East of the Indian Ocean. Contour lines by 0.04 (dashed contours for negatives values, grey colours for positive).*

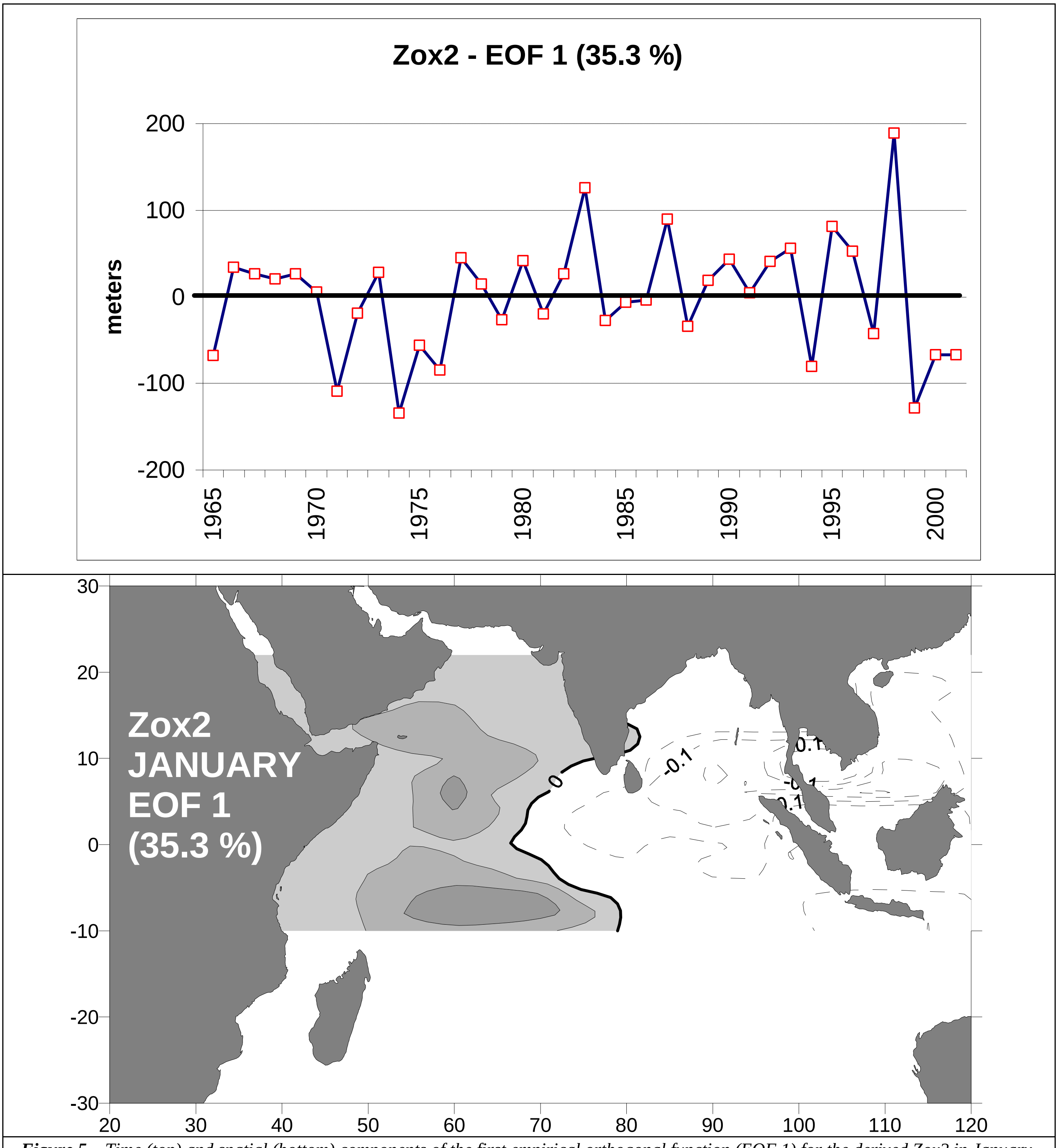

***Figure 5** – Time (top) and spatial (bottom) components of the first empirical orthogonal function (EOF 1) for the derived Zox2 in January, explaining 35.3 % of the variance of the anomaly field. This analysis explains the interannual variability for a given month, between 1965 and 2001. Contour intervals by 0.05. (dashed contours for negatives values, grey colours for positive).*

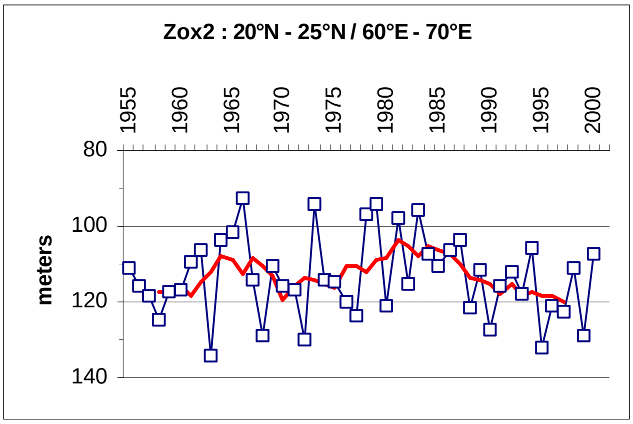

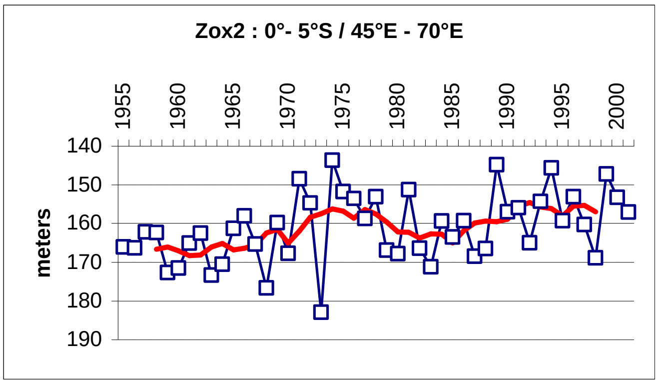

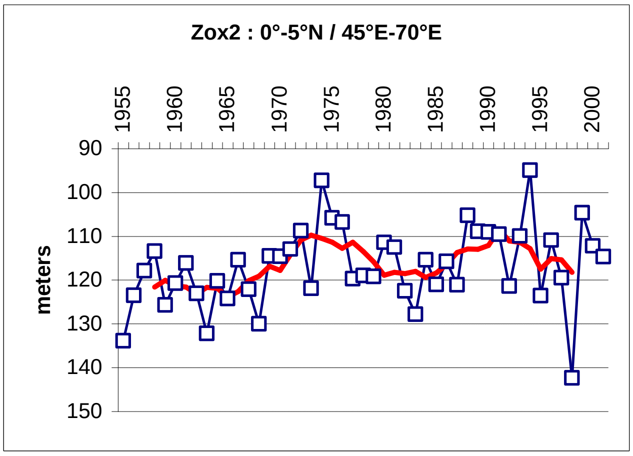

Figure 6 *- Time series of the depth of the 2 ml/l dissolved oxygen content in three yellowfin fishing areas : North of the Arabian Sea (May) (top panel) and Equatorial region (January) (lower panel)*